Front. Biol. China (2006) 2:203–207
DOI 10.1007/s 11515-006-0019-6

RESEARCH ARTICLE

Luo Chunxiong, Mao Yongdong, Ouyang Qi

DNA duplex membrane effect for the electrochemical detection of single-base DNA mutations

Abstract Here we report a new method to detect DNA point mutations. The method is based on the formation and deformation of double-stranded DNA (dsDNA) membranes on a gold surface. It can encage reporter molecules between the gold surface and the double-stranded DNA or keep them away from the gold surface. In these systems, $Fe(CN)_6^{3-}$ was used as the reporter. As the temperature increases, a sharp electrochemical signal change in the melting curve of wild-type dsDNA appears. At a special temperature, the method gives 100:1 selectivity for the perfect complement and single base mutation target. Thus, the system provides a simple and sensitive method to detect DNA point mutations without labeling targets.

Keywords membrane effect, nano-compartment, single mutation, electrochemistry

1 Introduction

DNA mutations detection has become widely used in clinical laboratory testing for genetic and infectious diseases (Tyagi et al., 1998). Certain technologies are based on the immobilization of single-stranded DNA (ssDNA) probes onto different physicochemical transducers, which convert the hybridization event into different measurement signals. Among those measurements, the electrochemical method has received a great deal of attention because of the considerable promises for rapid and low-cost DNA testing in the fields of merging DNA-chip and electronics technology (Kelley et al., 1999; Boon et al., 2000; Drummond et al., 2003; Mao et al., 2003). In our recent studies, the DNA nanocompartment model has been reported on DNA sequence detection (Mao et al., 2004). This method uses the molecular encaging effect of dsDNA membranes, which exhibits reversible changes in molecular mechanical properties. By using the encaged molecule as a hybridization indicator, sudden membrane forming-deforming transitions were observed, which substantially sharpened the melting profiles of the double-stranded DNA array. In those experiments, Methylene Blue (MB^+) was used as the redoxactive reporter. Whether anions can also be encaged in the compartment, however, remains unclear.

$Fe(CN)_6^{3-}$ has been used as the redoxactive reporter to determine if the well-assembled octadecyl mercaptam monolayers had the pinhole defect fraction (Diao et al., 1999), and to check if there is a high surface coverage of DNA duplexes (Kelley and Barton 1997). Hiroshi et al. also used it to perform the electrochemical detection of one base mismatch in an oligonucleotide (Aoki et al., 2000; Aoki and Umezawa 2002). It is well known that anions such as $Fe(CN)_6^{3-}$ do not associate with the dsDNA helices, making them electrochemically silent on the well-modified DNA surface. In our experiments, we used the DNA duplex membranes to insulate the gold surface from the redoxactive substances in the electrochemical measurement solution (Fig. 1). With the denaturation of DNA duplexes, the dsDNA membranes turned into an ssDNA monolayer, and the $Fe(CN)_6^{3-}$ in the electrochemical measurement solution were easily diffused onto the gold surface, providing pronounceable electrochemical signals. In another experiment, we used the DNA nano-compartment to encage $Fe(CN)_6^{3-}$ (Fig. 2). The $Fe(CN)_6^{3-}$ captured in the switchable DNA compartment was used as the electrochemical indicator to indicate the hybridization on electrode surface. In both experiments, we studied the melting curves for the perfectly complementary targets and the those with a single-base mutation. The electrochemical

Translated from *Acta Biophysica Sinica* 2005, 21（2）[译自：生物物理学报，2005,21(2)]

Luo Chunxiong, Mao Yongdong, Ouyang Qi (✉)
Laboratory for Biophysics and Biotechnology, Department of Physics, Beijing 100871, China
E-mail: qi@pku.edu.cn
Ouyang Qi
Center for Theoretical Biology, Peking University, Beijing 100871, China

responses display great differences between fully complementary and single-mismatch target. The results reveal that the dsDNA membrane effect can be used to detect single-base mismatch.

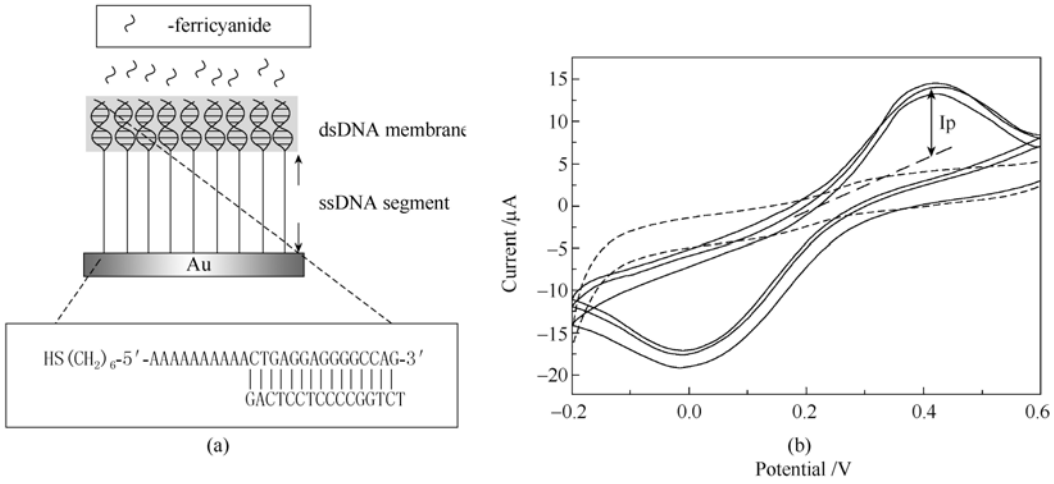

(**a**): shows the separating experiment when the membrane of DNA duplexes forms on gold surface;
(**b**): cyclic voltammogram for ssDNA modified electrode(line) and DNA duplexes well modified electrode(dots).The initial voltage was 0.6V and the end voltage was –0.2V, the scan rate was 0.1V/s, with a sample interval of 0.001V and sensitivity of 10^{-6}A/V. The value of I_p was defined as the difference between the reduction peak current and the baseline current (dashed line). The three cycles of cyclic voltammogram of ssDNA electrode show that I_p was relatively stable.

Fig. 1 Voltammetric behavior of $Fe(CN)_6^{3-}$ at DNA-modified gold electrodes

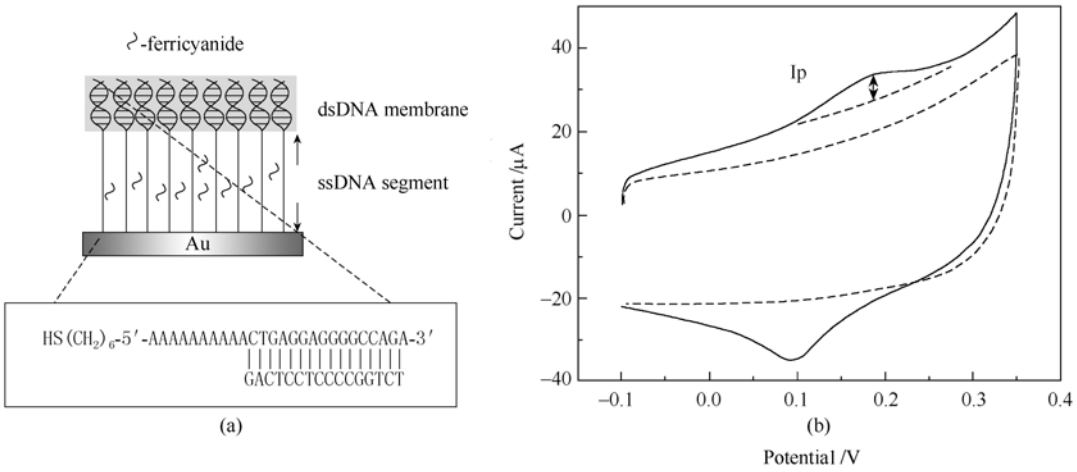

(**a**): shows the encaging experiment when the membrane of DNA duplexes surfaces form on the gold surface;
(**b**): cyclic voltammogram for DNA duplexes well modified electrode. The initial voltage was –0.1V and the end voltage was 0.35V, the scan rate was 1V/s. The value of I_p was defined as the difference between the reduction peak current and the baseline current (dashed line).

Fig. 2 The use of dsDNA nano-compartment to encage the $Fe(CN)_6^{3-}$

2 Materials and methods

2.1 Materials

All synthetic oligonucleotides were obtained from Sangon. Sequence A (HS-5' $(A)_9$CTG AGG AGG GGC CAG A3') has 9 adenines as spacers and a thiol group linked to the 5' phosphate end via a $(CH_2)_6$ spacer. Sequence B (5'TCT GGC CCC TCC TCA G3') is complementary to sequence A. Sequence C (5'TCT GGC CAC TCC TCA G3') has a point mutation (under bar) compared to sequence B.

2.2 Pretreatment of gold electrodes

Gold electrodes (the geometrical surface area is 0.1 cm^2) were polished with 0.05 μm alumina, and rinsed with ethanol and double distilled water at least three times. After sonication in ethanol for 20 min, the electrodes were etched in a solution (70% sulfuric acid, 30% peroxide) for about 15 min. Finally the electrodes were taken out and rinsed with

ethanol before placing it into clean tubes deoxygenated by pure N_2.

2.3 Preparation of single stranded DNA modified electrodes

Formation of the DNA duplexes solution was carried out by hybridization of 200nM of sequence A and 200 nM of sequence B in Tris-HCl (pH = 8.0) for 3~4 h at room temperature. Pretreated electrodes were then modified by incubation in 50 μL DNA duplexes solution for not less than 24 h at 4 ˚C. After which, electrodes were washed by wrea of a high concentration (30% in H_2O) to obtain single stranded DNA (ssDNA) modified electrodes. These ssDNA modified electrodes can be stored in the solution of TH / Tris-HCl at 4˚C for a long time.

2.4 Electrochemistry

All electrochemical experiments were performed using an electrochemical workstation model 660 (CH instruments Inc. USA).

When we used cyclic voltammetry (CV) to address the $Fe(CN)_6^{3-}$ confined on the gold surface, the peak current in the resulting voltammogram is given by :

$$i_p = \frac{n^2F^2}{4RT} v \cdot A \cdot \Gamma \quad (1)$$

here, n is the number of electrons per molecule for redox reaction, F is the Faraday constant, R is the gas constant, T is the temperature, v is the potential scan rate, A is the electrode area. Γ is the surface concentrations of $Fe(CN)_6^{3-}$ encaged by the membrane of the DNA duplexes. This equation provides a means to determine Γ approximately.

3 Results and discussion

3.1 The dsDNA surface density on the gold surface

It has been reported that the coverage of oligonucleotide attached to gold surface is related to its attachment concentration and reaction duration (Herne and Tarlov 1997; Kelley and Barton 1997). Our atomic force microscopy (AFM) study showed that the coverage of the dsDNA SAM under our experimental condition was about $5.4 \pm 0.8 \times 10^{12}$ molecules / cm (Mao et al., 2004).

In our experiment, after the hybridization of fluorescein labeled wild-type DNA to the ssDNA-modified electrode, we rinsed the electrode with Tris buffer (contain 1mM $MgCl_2$). Then we put the electrode in 50μL double distilled water at 90˚C for 10 min. From the fluorescein concentration of the 50μl solution washed from the electrode (Table 1), we could calculate that fluorescein-dsDNA surface density (about $5 \pm 2 \times 10^{12}$ molecules / cm^2). It was consistent with the AFM results(Mao et al., 2004) and other papers (Herne and Tarlov 1997; Kelley and Barton 1997).

Table1 Using the solution washed from Fluorecein-DNA modified electrode to calculate the DNA surface density.

Electrode numbers	1	2	3
The CCD counts of solution washed from electrode	1100	1500	980
The known concentration of fluorescein solution /nM	7.5	15	30
CCD(counts)	550	1300	2500

3.2 Voltametric behavior of $Fe(CN)_6^{3-}$ at DNA-modified gold electrodes

The voltammetry of the $Fe(CN)_6^{3-}$ at our DNA-modified electrodes offered qualitative information on the system organization (Fig. 1). The voltammograms of $Fe(CN)_6^{3-}$ at ssDNA-modified electrode and dsDNA-modified electrode were given in Fig. 1(b). We observed that the CV curve of ssDNA-modified electrode was in a reversible surface wave format. Because the negative charge of high density ssDNA probe modified surface, the peak of redox reaction had a movement ($\Delta E_p > 350$ mV). The curve of dsDNA-modified electrode (dashed line) was in a capacitive format. The CV behavior of the dsDNA-modified electrode was in good agreement with previous reported data (Hashimoto et al., 1994; Steel et al., 1998; Yang et al., 1998).

3.3 Using $Fe(CN)_6^{3-}$ in the electrochemical solution to monitor the melting curve of dsDNA modified electrode

We monitored the electrochemical signal changes of wild-type dsDNA-modified electrode as a function of temperature from 25˚C to 60˚C in the solution that contained 2 mM $Fe(CN)_6^{3-}$. The same measurement was performed on the electrode modified with single-base mismatched dsDNA and the one modified with ssDNA. Results are summarized in Fig. 3. The CV electrochemical signal I_{peak} of wild-type dsDNA-modified electrode remained almost unchanged when temperature was below 45 ˚C; it suddenly increased from 0.4 ± 0.2 A to 8.1 ± 0.2 A as the temperature was raised from 45˚C to 50 ˚C. On the other hand, the electrochemical signals on the electrode modified with single-base mismatched dsDNA and the one

modified with ssDNA remained consistent (8.4±0.2 A) within the temperature range of 20 ˚C to 60 ˚C.

The melting temperature of the wild-type DNA duplexes was 52.6˚C. When more than 35% dsDNA was de-hybridized, the dsDNA membrane deformed and Fe $(CN)_6^{3-}$ in the electrochemical solution could easily reach the gold surface, causing a sharp increased in the electrochemical signal. Our experiments showed that the characteristic hybridization efficiency was 65 ± 5%, below which the dsDNA membrane would leak. We regard there is no obvious redox peak on the dsDNA modified electrode not only for the negative charge of dsDNA (Aoki et al., 2000; Aoki and Umezawa 2002), but also for the size of dsDNA array and the reporter molecules.

For the target with single-base mismatch, the measurement of quartz crystal microbalance showed that the efficiency of hybridization was less than 50% (Okahata et al., 1998). Thus it cannot construct a well-formed dsDNA membrane. In this case, the reporter molecules (Fe $(CN)_6^{3-}$) could freely diffuse onto the gold surface, so that the electrochemical signal remained high (Fig. 3). From the two melting curves, we can differentiate the perfectly complementary target from single-base mutation target.

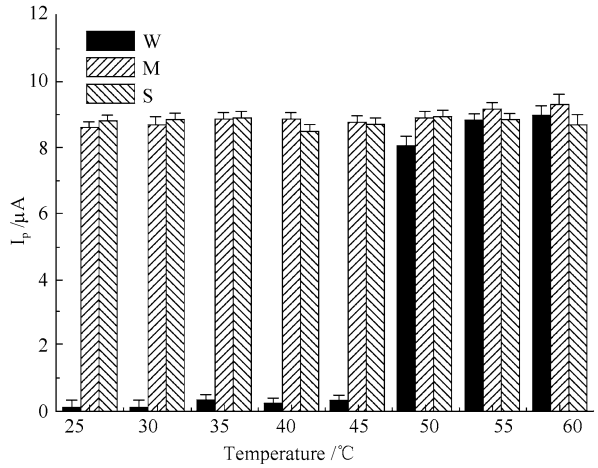

The measurements of I_p as a function of temperature for different DNA modified electrodes. The solution of the electrochemical measurement is Tris-HCL (pH8, containing 1mM $MgCl_2$, 0.1M KCl and 2mM $K_3Fe(CN)_6$). The CV scan ranges from –0.2V to 0.6V, and the scan rate is 0.1V/s. W means the probe hybridized to the wild type segment, M means the single-base mismatch probe and the S refers to the single-strand one.

Fig. 3 Using $Fe(CN)_6^{3-}$ in the electrochemical solution to monitor the melting curve of dsDNA modified electrode

3.4 The use of dsDNA nano-compartment to encage the Fe $(CN)_6^{3-}$

$K_3Fe(CN)_6$ was not added to the electrochemical solution but to the hybridization solution. After 12 h of hybridization, the peak shape CV electrochemical signal can be obtained. We also carried out the same experiment for the ssDNA-modified electrode and results showed that it is electrochemically silent (Fig.2). Using equation (1) (see section on Materials and methods), we could calculate the quantity of the encaged $Fe(CN)_6^{3-}$ according to the electrochemical signal. The relationship between the encaged $Fe(CN)_6^{3-}$ surface density Γ and the $Fe(CN)_6^{3-}$ concentration of hybridization solution fits the Langmuir isotherm (Steel et al., 1998) (Fig. 4): $[Fe(CN)_6^{3-}] / \Gamma = (1 / \Gamma_{max}) [Fe(CN)_6^{3-}] + (1 / K\Gamma_{max})$, where K is the association constant per site. Our experimental data gives the association constant $0.9 \pm 0.1 \times 10^3$ M^{-1} for $Fe(CN)_6^{3-}$. This is much smaller than the association constant for a positively charged molecule MB^+, which was reported as $3.0 \pm 0.2 \times 10^4$ M^{-1} (Mao et al., 2004).

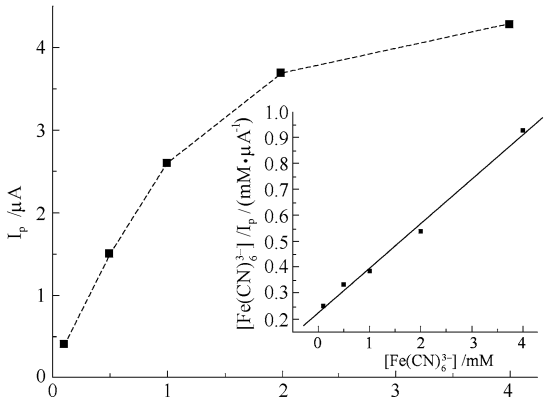

$[Fe(CN)_6^{3-}]$ = 0.1, 0.5, 1, 2, and 4 mM. The scan rate is 1 V/s. Inset is a fit of the data to the Langmuir adsorption isotherm.

Fig. 4 The I_p of Cyclic voltammetry vs different $[Fe(CN)_6^{3-}]$ concentration that contained in the hybridized solution

We monitored the I_{peak} as a function of temperature after the DNA nano-compartment had captured Fe $(CN)_6^{3-}$. Results are shown in Fig. 5. For the wild-type dsDNA membrane, I_{peak} remained the same value 4.5 ± 0.2 A from

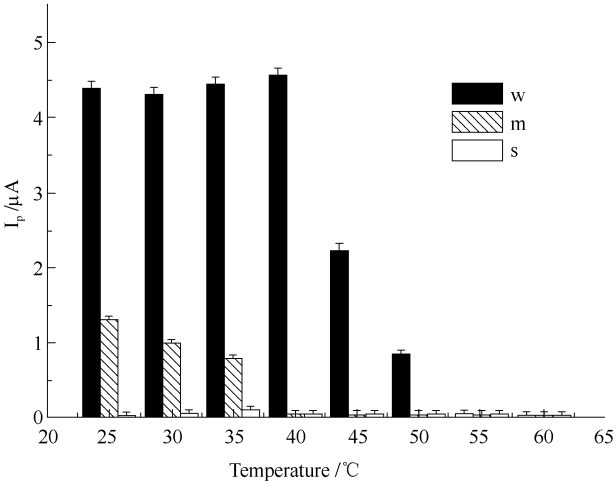

W means the probe hybridized to the wild type segment, M means the single-base mismatch and S refers to single-strand one. The range of CV is from – 0.1V to 0.35V. The concentration of $Fe(CN)_6^{3-}$ of the hybridization solution is 4mM.

Fig. 5 The measurements of I_p as a function of temperature for different DNA modified electrodes in encaging experiment

25˚C to 40˚C. It continuously decreased from 4.5 ± 0.2 × 10^{-6}A to 0.2 ± 0.2A (regarded as 0) as the temperature raised from 40˚C to 55˚C. For the single-base mismatch (sequence C) hybridized probe, I_{peak} was much smaller than that of the wild-type. Furthermore, the temperature when the I_{peak} was decreased to zero was about 40˚C, and was much lower than the melting temperature of wild-type hybridized probe. I_{peak} of the ssDNA modified electrode remained zero (less than 0.2 A) from 25˚C to 60˚C. When a spacer composed of 9 adenine bases between dsDNA and gold surface was used, the signal obtained from few Fe $(CN)_6^{3-}$ binding with DNA could be neglected due to the low electron transport efficiency through the long spacer (Kelley and Barton 1992). Thus, the difference between the curves of Fig. 5 was due to different concentrations of encaged Fe $(CN)_6^{3-}$ on the gold surface. In these experiments, we found that the encaged Fe $(CN)_6^{3-}$ of the wild-type probe modified electrode was at least three times more than the mutation probe modified electrode at room temperature, and 20 times more than that at 40˚C.

From the percent encaged indicator *vs*. temperature curve (Fig. 5), we find that the encaged Fe $(CN)_6^{3-}$ started to flow away when the hybridization efficiency was less than 80%. The membrane was totally deformed when the hybridization efficiency was less than 30%. The difference of characteristic hybridization efficiency between encaging and insulating effects of the dsDNA membrane may be attributed to the fact that the former is the local surface effect while the latter is the whole surface effect.

4 Conclusions

The advantage of our DNA probe lies in the collective effect of the dsDNA membrane, which is highly sensitive to detect single-base DNA mutations. In this work, we use dsDNA membrane to show not only the insulating effect but also the encaging effect of dsDNA membrane. The methods described above hold great promise for detection of known mutations within defined sequences and sequencing assays. Our experimental results give 20:1 selectivity, while the fluorophore-base system has 2.6:1 selectivity even at its optimum stringency temperature (42˚C). With this technique, the detection limit for the probe is proportional to the area of DNA modified surface. The surface area of our electrode is 0.1 cm^2, and our experiments show that it can detect ~10^{11} DNA molecules. Extrapolating from this result, a 100 μm^2 electrode is possible to detect ~10^6 molecules (Mao et al., 2004). Therefore, this label-free and PCR-free DNA detection method may greatly simplify the protocol of a DNA chip compared to conventional methods. It even has the potential to detect in vivo DNA or RNA in real time, whereas the label-dependent methods cannot afford to finish this task.

Acknowledgements This work was supported by Hi-Tech Research and Developmont Program of China (No.2002AA221011)

References

Tyagi S., Bratu D.-P., Kramer F.-R., Multicolor molecular beacons for allele discrimination, Nat. Biotechnol., 1998, 16: 49–53

Mao Y.-D., Luo C.-X., Ouyang Q., Studies of temperature-dependent electronic transduction on DNA hairpin loop sensor, Nucleic Acids Res., 2003, 31: No18 e108

Boon E.-M., Ceres D.-M., Drummond T.-D., Hill M.-G., Barton J.-K., Mutation detection by electrocatalysis at DNA-modified electrodes, Nat. Biotechnol., 2000, 18: 1096–1100.

Kelley S.-O., Boon E.-M., Barton J.-K., Jackson N.-M., Hill M.-G., Single-base mismatch detection based on charge transduction through DNA, Nucleic Acids Res.,1999,27: 4830–4837

Drummond T.-G., Hill M.-G., Barton J.-K., Electrochemical DNA sensors, Nat. Biotechnol., 2003, 21: 1192–1199

Mao Y.-D., Luo C.-X., Deng W., Jin G.-Y., Yu X.-M., Zhang Z.-H., Ouyang Q., Chen R.-S., Yu D.-P., Reversibly switchable DNA nanocompartment on surface, Nucleic Acids Res., 2004, 32: 19e144

Diao P., Jiang D.-L., Cui X.-L. Gu D.-P., Tong R.-T., Zhong B., Studies of structural disorder of self-assembled thiol monolayers on gold by cyclic voltammetry and ac impedance, J. Electroanal. Chem., 1999, 464: 61–67

Kelley S.-O., Barton J.-K., Electrochemistry of methylene blue bound to a DNA-modified electrode, Bioconjug. Chem., 1997, 8: 31–37

Aoki H., Buhlmann P., Umezawa Y., Electrochemical detection of a one-base mismatch in an oligonucleotide using ion-channel sensors with self-assembled PNA monolayers, Electroanalysis, 2000, 12: 1272–1276

Aoki H., Umezawa Y., High sensitive Ion-Channel sensors for detection of oligonucleotides using PNA modified gold electrodes, Electroanalysis, 2002, 14: No.19–20

Herne T.-M., Tarlov M.-J., Characterization of DNA probes immobilized on gold surfaces, J. Am. Chem. Soc, 1997, 119: 8916–8920

Steel A.-B., Herne T.-M., Tarlov M.-J., Electrochemical quantitation of DNA immobilied on gold, Anal. Chem., 1998, 70: 4670–4677

Yang M., Yau H.-C.-M., Chan H.-L., Adsorption kinetics and ligand-binding properties of thiol-modified double-stranded on a gold surface, Langmuir, 1998, 14: 6121–6129

Hashimoto K., Ito K., Ishimorl Y., Sequence-specific gene detection with a gold electrode modified with DNA probes and an electrochemically active dye, Anal. Chem., 1994, 66: 3830–3833

Okahata Y., Kawase M., Nikura K., Ohtake F., Furusawa H., Ebara Y., Kinetic measurement of DNA Hybridization on an oligonucleotide-immobilized 27-MHz quartz crystal microbalance, Anal. Chem., 1998, 70: 1288–1296

Kelley S.-O. and Barton J.-K., Electron transfer between bases in double helical DNA, Science, 1999, 283: 375–381